Drug Development and Industrial Pharmacy

ISSN: 0363-9045 (Print) 1520-5762 (Online) Journal homepage: http://www.tandfonline.com/loi/iddi20

A novel mixed polymeric micelle for co-delivery of paclitaxel and retinoic acid and overcoming multidrug resistance: synthesis, characterization, cytotoxicity, and pharmacokinetic evaluation

Jaber Emami, Mahboubeh Rezazadeh, Mahboubeh Mashayekhi, Mahboubeh Rostami & Ali Jahanian-Najafabadi

To cite this article: Jaber Emami, Mahboubeh Rezazadeh, Mahboubeh Mashayekhi, Mahboubeh Rostami & Ali Jahanian-Najafabadi (2017): A novel mixed polymeric micelle for co-delivery of paclitaxel and retinoic acid and overcoming multidrug resistance: synthesis, characterization, cytotoxicity, and pharmacokinetic evaluation, Drug Development and Industrial Pharmacy, DOI: 10.1080/03639045.2017.1411940

To link to this article: https://doi.org/10.1080/03639045.2017.1411940

Accepted author version posted online: 13 Dec 2017.

A novel mixed polymeric micelle for co-delivery of paclitaxel and retinoic acid and overcoming multidrug resistance: synthesis, characterization, cytotoxicity, and pharmacokinetic evaluation

Jaber Emami

Department of pharmaceutics, School of pharmacy and pharmaceutical science, Isfahan university of medical science, Isfahan, Iran

Mahboubeh Rezazadeh (corresponding author)

Department of pharmaceutics and novel drug delivery system research center, School of pharmacy and pharmaceutical science, Isfahan university of medical science, Isfahan, Iran

Tel: (031) 37927123

Fax: (0311) 668-0011

E-mail: rezazade@pharm.mui.ac.ir

Mahboubeh Mashayekhi

Department of pharmaceutics, School of pharmacy and pharmaceutical science, Isfahan university of medical science, Isfahan, Iran

Mahboubeh Rostami

Department of Medicinal chemistry, School of pharmacy and pharmaceutical science, Isfahan university of medical science, Isfahan, Iran

Ali Jahanian-Najafabadi

Department of Pharmaceutical Biotechnology, Isfahan University of Medical Sciences, School of pharmacy and pharmaceutical science, Isfahan university of medical science, Isfahan, Iran

Abstract

In the current study, retinoic acid (RA) was conjugated to Pluronic F127 (PF127) through an esterification process. Mixed micelles were formed with tocopheryl polyethylene glycol 1000 (TPGS) for co-delivery of paclitaxel (PTX) and RA to the cancer cells. Mixed micelles of RA-PF127 and TPGS in different weight ratios (10:0, 7:3, 5:5, 3:7, 0:10 w/w) were prepared and physicochemical properties including, particle size, zeta potential, critical micelle concentration (CMC), drug loading content, entrapment efficiency, drug release, cellular uptake and in vitro cytotoxicity, were investigated in details. Furthermore, the pharmacokinetics of PTX-loaded optimized mixed micelles were evaluated in Sprague-Dawley rats and compared with Stragen® (PTX in Cremophor EL®). Particle sizes and zeta potentials of the drug-loaded micelles were in the range of 102.6–223.5 nm and -5.3 to -9.6 mV, respectively. The 7:3 and 5:5 micellar combinations had lower CMC values (0.034 - 0.042 mg/mL) than 0:10 (0.124 mg/mL). The entrapment efficiencies of 10:0, 7:3, and 5:5 were 53.4 ± 9.3 %, 61.3 ± 0.5 %, and 78.7 ± 1.66 %, respectively. The release rates of PTX from 7:3 and 5:5 mixed micelles were significantly slower than other formulations. Cytotoxicity assay demonstrated increased cytotoxic activity of PTX-loaded mixed micelles compared to free PTX. The V_d and $t_{1/2ß}$ of PTX-loaded RA-PF127/TPGS (7:3) were increased by 2.61- and 1.27-fold, respectively, while the plasma AUC of the micelles was 2.03-fold lower than those of Stragen®. Therefore, these novel mixed micelles could be effectively used for delivery of PTX and RA to the cancer cells. Moreover, TPGS as part of micelle composition could enhance the therapeutic effect of PTX and reduce side effects.

Introduction

Although different effective techniques have so far been evaluated in the last decades, chemotherapy is still being widely used in the treatment of cancers [1-3]. Combination chemotherapy using two or more drugs compared to single-agent chemotherapy, has some unique advantages such as signaling different pathways, improving therapeutic efficacy, and suppressing and reversing drug resistance [3]. Recent studies on combination chemotherapy has focused on searching for less cytotoxic drugs. In this regard, retinoic acid (RA), a natural derivative of vitamin A, has attracted attention as an effective anticancer agent [4, 5]. Cell growth inhibition activity of RA is not attributed to a general cytotoxicity; rather RA is proposed to control progression of cancer by induction of cell differentiation, inhibition of cell proliferation, anti-migration and anti-invasion activity against cancer cells [5]. RA has been shown to inhibit the growth of human breast cancer cell line, MCF-7, in concentrations greater than10 nM in cell culture medium [4]. Other studies have also proven that RA inhibits the growth of hepatocellular carcinoma[6]. Some clinical trials have demonstrated the chemopreventive effect of RA [7, 8]. For example, addition of RA as an adjutant, considerably inhibited the development of second primary cancers in patients with early stage of skin, breast, hepatocellular, head and neck cancers [7]. A literature survey indicated that RA and its derivatives synergistically act with anticancer drugs such as doxorubicin, cisplatin, and paclitaxel (PTX) to induce receptor-mediated apoptosis and suppress cell survival factors [9-11]. Therefore, combination of RA with other conventional cytotoxic drugs enhance therapeutic efficacy and reduce side effects compared to single chemotherapy. Nevertheless, the clinical application of RA is restricted due to its poor water solubility, physicochemical instability, potential systemic side effects, and lack of an efficient delivery strategy. Drug delivery systems such as liposome [12] , polymeric [13] and solid lipid nanoparticles [14, 15] have so far been evaluated for delivery of RA to the cancerous cells. However, the loading pay off of RA is often inadequate and unstable, as most of the drug is easily leaked out from carriers during storage or after injection into the blood stream. Recently, a hybrid nonocarrier known as polymer-oil nanostructured carrier was developed to solubilize RA and to provide a more stable delivery system for this agent [16]. Although this novel carrier exhibited higher anti-tumor activity than free RA, the preparation of the formulation is so complicated and due to the low solubilizing efficiency, this formulation could not be used for co-delivery of RA with other lipophilic anticancer agents. In some studies, in order to increase loading capacity and to control the release rate, RA has been chemically conjugated to different polymers [17, 18]. For instance, in the work of Zhang, *et al*., RA was conjugated to chitosan oligosaccharide to form polymeric nanoparticles facilitating the co-delivery of RA and PTX [18]. However, based on *in vitro* cytotoxicity study, RA-conjugated-chitosan

nanoparticles did not show any significant cytotoxicity even at the highest concentration, which was attributed to the low degree of RA conjugation to the chitosan oligomer. In the current study, we developed a novel polymeric micelle through conjugation of Pluronic F127 (PF127) to RA to form mixed micelles with tocopheryl polyethylene glycol 1000 (TPGS) for co-delivery of PTX and RA. Pluronic block copolymer consists of ethylene oxide (EO) and propylene oxide (PO) blocks that are arranged in a basic EO*x*–PO*y*–EO*x* structure. A prominent feature of Pluronic copolymer is the ability to form a core-shell structure in aqueous media, providing a hydrophobic space in the core where hydrophobic drugs can be solubilized, while the hydrophilic corona maintains the dispersion stability of Pluronic micelles [19]. In the present study, RA was conjugated to the Pluronic via esterification process and mixed micelles formed with TPGS which then loaded with PTX. TPGS is a water-soluble derivative of natural Vitamin E, which is synthesized by esterification of α-tocopheryl succinate (α-TS) with polyethylene glycol 1000 (PEG) and has been approved by FDA as a safe pharmaceutical adjuvant used in drug formulation [20]. TPGS has an amphiphilic structure which forms micelles in aqueous media. PTX has a high solubility in α-TS (11 mg/mL) which enhances polymer–drug miscibility thereby improving drug loading into the micelles [21]. TPGS is regarded as an excipient which inhibits drug efflux pumps or p-glycoproteins (p-gp) overcoming multidrug resistance [22-24] . Tumors usually consist of mixed populations of malignant cells some of which seem to show drug sensitivity while other appear to be resistance. Chemotherapeutic drugs may kill all sensitive cells but leave behind a higher proportion of drug resistance cells. TPGS by inhibiting p-gp overexpressed on the surface of malignant cells could facilitate permeation of the drugs to the cells, leading to increased cytotoxicity and bioavailability of antitumor agents. In addition, TPGS could effectively inhibit the growth of cancer cells by its ability to induce apoptosis [23-25]. Thus, it can be assumed that incorporation of TPGS in delivery system could greatly enhance the therapeutic effects of the formulated anticancer drugs. Moreover, the drug release profile could be precisely controlled by adjusting the quantity of RA-PF127 and TPGS in the carrier. Therefore, this work focuses on synthesis of RA- PF127 derivative, development and *in vitro* assessment of mixed micelles of RA-PF127/TPGS loaded with PTX including particle size, zeta potential, release properties, and storage stability. Furtheremore, we evaluated cellular uptake and synergistic cytotoxic effect of the drug-loaded mixed micelles against human breast cancer cell line, MCF-7. Moreover, the pharmacokinetics of PTX-loaded micelles were estimated in Sprague-Dawley rats and compared with Stragen® (PTX in Cremophor EL®).

Materials and methods

Materials

Pluronic F127 (PF127, molecular weight: 12.5 KD) and retinoic acid (RA) were provided from Sigma–Aldrich (St. Louis, MO, USA). α-Tocopheryl polyethylene glycol 1000 succinate (TPGS) was purchased

from Eastman Co. (USA). Paclitaxel (PTX), dicyclohexylcarbodiimide (DCC), 4-(dimethylamino) pyridine (DMAP), pyrene, anhydride dimethyl sulfoxide (DMSO), dichloromethane, ethanol, and fluorescein isothiocyanate (FITC) were purchased from Sigma Chemical Co. (St. Louis, MO). Orthophosphoric acid and potassium dihydrogen phosphate were obtained from Merck (Germany), HPLC grade methanol and acetonitrile were supplied by Caledon (Ontario, Canada). Paclitaxel Stragen® (30 mg/5 ml) was provided by Sobhan Oncology (Rasht, Iran). Roswell Park Memorial Institute (RPMI)-1640 medium, fetal bovine serum (FBS) and antibiotics for cell culture were provided by Sigma–Aldrich (St. Louis, MO). Human breast cancer cell line (MCF-7) was obtained from Pasteur institute (Tehran, Iran). 3-(4,5-Dimethylthiazol-2-yl)-2,5-diphenyltetrazolium bromide (MTT) was supplied by Sigma–Aldrich.

Animals

Sprague-Dawley rats (5–6 weeks old, 200–250 g body weight) were obtained from the laboratory animal center of the Faculty of Pharmacy and Pharmaceutical Science, Isfahan University of Medical Science, Isfahan, Iran. Animals were pathogen free and allowed free access to food and water. All animal experiments were carried out in accordance with Guide for the Care and Use of Laboratory Animals published by the National Institute of Health which approved by the research ethics committee of Isfahan University of Medical Science (ethical approval code 294189) .

Synthesis of RA-PF127 derivative

RA- PF127 copolymer was synthesized via the reaction of activated carboxyl group of RA with hydroxyl group of PF127 in the presence of DCC and DMAP. Briefly, RA (0.2 mmol, 60.1 mg), DCC (49.5 mg, 0.24 mmol), and DMAP (24.5 mg, 0.2 mmol) were dissolved in anhydrous DMSO and stirred under nitrogen for 24 h in dark to activate the carboxyl group of RA. The solution of PF127 (500 mg 0.04 mmol) in DMSO was added into the activated RA solution and the reaction mixture was stirred for 48 h under nitrogen. The mixture was then dialyzed against ethanol for 48 h to remove unreacted RA, followed by dialysis against water for 24 h using dialysis membrane (molecular weight cutoff (MWCO): 2 kDa, Viskase Companies Inc., Darien, IL) and lyophilized to get pure RA-PF127 powder (Freeze Dryer Model ALPHA 2-4 LD plus, Christ Company, Stuttgart, Germany). The chemical structure of RA-PF127 was identified and calculated by ^{1}H-NMR (Bruker, Biospin, AC-400, Mannheim, Germany) and Fourier transform infrared (FT-IR) (WQS-510/520, Raileigh, China) spectra. ^{1}H NMR spectrum was also used to determine the degree of substitution (DS) or the molar ratio of RA grafting to PF127.

Preparation of the blank and PTX-loaded micelles

To prepare empty mixed micelles, RA-PF127 alone or in mixture with TPGS at different weight ratios (10:0 to 0:10 w/w) was dissolved in dichloromethane and the organic solvent was then removed by rotary vacuum evaporation. The resultant film was hydrated with a suitable volume of deionized water, incubated at 37 ºC for 30 min, and then sonicated for a few minutes. The micellar solution was centrifuged at 7000 rpm for 10 min, and filtered through a 0.45 µm pore size microfiltration membrane [26]. PTX-loaded polymeric micelles were prepared by dissolving 3 mg PTX in dichloromethane which was then added to 10 mg polymer mixture already dissolved in dichloromethane. The micelle preparation steps described above were exactly repeated. The drug-loaded micelles were lyophilized and kept at 4◦C until further evaluations.

Characterization of the micelles

Measurement of particle size and zeta potential

The average hydrodynamic diameters and zeta potentials of the mixed micelle solutions (1 mg/mL) in phosphate buffer saline (PBS, pH 7.4) were measured with dynamic light scattering (DLS) using a ZetaSizer (3000HS, Malvern Instruments Ltd., Malvern, UK). All measurements were carried out at 25 ºC and performed in triplicate.

Determination of critical micelle concentrations

Critical micelle concentration (CMC) was determined by a fluorescence probe technique using pyrene as a fluorescence probe [27]. Briefly, 2 mg/mL of the polymer mixtures at different weight ratios were prepared in dichloromethane. Different volume of these solution was added to 15-mL empty vials. Then 1 mL of 6×10^{-6} M solution of pyrene in dichloromethane was added in every vial and mixed well. The dichloromethane was left to evaporate for 24 h in order to form a pyrene film in the vial. Finally,10 mL deionized water was added to the vials to obtain a final pyrene concentration of 6×10^{-7} M for each vial and the polymer solutions with concentrations ranging from 0.003 mg/mL to 0.5 mg/mL at different weight ratios . The solutions were kept on a shaker at 37 ºC for 24 h to reach equilibrium before fluorescence measurement. Fluorescence spectra were recorded with spectrofluorometer (Jasco FP 750, Tokyo, Japan) with the emission wavelength at 390 nm. From the pyrene excitation spectra, the intensity

ratio of the first peak (I_1, 331 nm) to the third peak (I_3, 339 nm) was plotted against the logarithm of polymer concentration. Two tangents were then drawn and the CMC values were taken from the intersection between the two tangents.

Determination of drug loading

To estimate the drug loading content, 2 mg of the lyophilized sample was dissolved in 25 mL of acetonitrile and the solution was ultrasonicated for 10 min to dissolve PTX-loaded micelles entirely. The resultant solution was filtered through 0.45 µm filter unit and PTX concentration was determined by HPLC method developed and validated in our laboratory [27]. Chromatographic separation was performed using a reversed-phase C_{18}-Bondapak (3.9 mm × 250 mm) HPLC column. The mobile phase consisted of potassium dihydrogen phosphate (0.01 M)/acetonitrile (52:48) with final pH adjusted to 4 ± 0.1 with orthophosphoric acid. The mobile phase eluted at 1.5 mL/min and the effluent was monitored at 227 nm using a UV detector. Column temperature was kept at 40 °C and 30 µL of the sample was injected into the HPLC column. The calibration curve constructed in the range of 0.25 – 12 µg/mL of PTX was linear (r^2> 0.998). The inter- and intra-day precision and accuracy of the assay were less than 15.87%. Drug entrapment efficiency (EE) and drug loading (DL) were calculated by following equations:

$$EE\% = \frac{\text{weight of the drug in the micelles}}{\text{weight of the feeding drug}} \times 100$$

$$DL\% = \frac{\text{weight of the drug in the micelles}}{\text{weight of the micelles}} \times 100$$

***In vitro* drug release studies**

The lyophilized powder of PTX-loaded micelles (2 mg) was dissolved in 2 mL of phosphate buffer solution (0.1 M, pH: 7.4). The resulting solution was placed in a dialysis bag (MWCO: 10 kDa), and the bag was immersed in a glass beaker with 100 mL phosphate buffer (0.1 M, pH: 7.4) containing 0.2 % tween 80 to provide sink condition with agitation of 100 rpm at 37 °C [28] . Sample aliquots were withdrawn from the release medium at pre-determined time intervals and replaced with fresh buffer. The content of PTX was determined by the above described HPLC method. Dissolution efficiency (DE) was used to compare the release rates amongst formulations. DE of release profiles were calculated from the

area under the curve at time t_j (measured using the trapezoidal rule) and expressed as the percentage of the area of the rectangle described by 100% dissolution in the same time [29]

Storage stability studies of the PTX-loaded mixed micelles

The lyophilized PTX-loaded RA-PF127/TPGS with weight ratio 7:3 and 5:5 were stored in sealed flasks at 4 ºC for three months. Afterward, the micelles were examined for the particle size and zeta potential, using a Zeta Sizer 3000HS instrument following protocol described earlier. Then the micellar solution was filtered through a 0.45-mm syringe filter to remove PTX that had aggregated due to its low solubility in water. The filtered micelle solution was analyzed by HPLC to determine the PTX concentration [21].

Cell culture

Human breast cancer cells, MCF-7, were maintained in RPMI 1640 supplemented with 10% (v/v) FBS and 1% penicillin–streptomycin at 37 ºC and 5% CO2. Cells were subcultured regularly using trypsin/EDTA.

Cellular uptake studies

FITC-labeled micelles (FITC/RA-PF127/TPGS, (7:3)) were prepared through the reaction between hydroxyl group of PF127 and isothiocyanate of FITC. Briefly, 2.7 mg/mL FITC solution in ethanol was prepared and 500 µL of this solution was dropped into the polymer solution. The molar ratio of the polymer to FITC was controlled at 1:1. The solution was stirred for 24 h at room temperature and in dark condition; the reaction product was dialyzed against deionized water using a dialysis membrane (MWCO: 8 kDa) for 24 h to remove the unreacted FITC [27] . Then, the dialyzed products were lyophilized to obtain FITC-labeled micelles.

In a 12-well culture plate, MCF-7 cells were seeded at a density of 2×10^5 cells per well in 2 mL of growth medium and incubated for 24 h to facilitate attachment. Cells were then incubated with FITC-labeled micelles at concentration of 20 µg/mL of the polymer at different times. Cells were washed twice with PBS (pH: 7.4) and directly observed under a fluorescence microscope (CETI, 3100.5000 Triton II, UK).

***In vitro* cytotoxicity assay**

The cytotoxicities of the free drug in DMSO, PTX-loaded RA-PF127/TPGS (7:3), PTX-loaded RA-PF127/ TPGS (5:5), PTX-loaded RA-PF127, blank RA-PF127/TPGS (7:3), RA-PF127/TPGS (5:5), RA-MTT assay. The cells were seeded at density of 3×10^4 cells/well in a 96-well culture plate (SPL Lifescience, Gyeonggi-Do, Korea). When the cell confluence reached 75%, the cells were incubated with

samples for 48 h at the equivalent PTX concentrations of 0.012–2.345 µM. After incubation, 20 µL of MTT solution (5 mg/mL in 0.02 M phosphate buffer) was added to each well and the plate was incubated for another 4 h. Subsequently, unreacted MTT and medium was removed and the formazan crystals in cells were dissolved in 150 µL of DMSO. The absorbance was measured at 570 nm using enzyme-linked immunosorbent assay plate reader (Stat Fax-2100; Awareness Technology Inc., Palm City, FL). Untreated cells were taken as the negative control with 100% viability and the blank culture medium was used as a blank control [30] . Cell viability for each sample was calculated using following equation.

$$Cell\ viability\% = \frac{\text{mean absorbance of each group} - \text{mean absorbance of blank}}{\text{mean absorbance of negative control} - \text{mean absorbance of blank}} \times 100$$

Pharmacokinetic studies

Twenty male Sprague Dawley rats (200-250 g) were used to investigate the effect of formulations on the pharmacokinetics of PTX after intravenous (i.v.) administration. Rats were randomly assigned into two groups of 10 each and injected intravenously through the tail vein with a single dose of PTX Stragen® or PTX-loaded RA-PF127/ TPGS (7:3) micelles at an equivalent dose of 7 mg/kg PTX per body weight. Blood samples (0.4 mL) were collected into heparinized tubes at 0 (predose), 5, 30 min, 1 , 2, 4, 8, and12 h after i.v. administration. The blood samples were centrifuged at 3000 rpm for 10 min to obtain the plasma and stored at −20 °C until analyzed for PTX.

Analysis of PTX

Plasma concentrations of PTX were determined using a reversed-phase HPLC method with UV detection developed and validated in our laboratory. Briefly, 50 µL of sodium acetate buffer (pH, 5), 30 µL of internal standard (25 µg/mL diazepam in methanol) and 6 mL of diethyl ether were added into 300 µL of plasma samples. Sample tubes were vortexed for 2 min and centrifuged at 5000 rpm for 10 min. The upper organic layer was transferred to the clean tubes and evaporated to dryness under nitrogen gas. The residue was reconstituted with 100 µL of mobile phase and 50 µL aliquot was injected into the HPLC column. Chromatographic separation was achieved using a reversed-phase C_{18}-Bondapak column (3.9 mm × 250 mm) at 58 °C. The mobile phase consisted of acetate buffer (0.01 M)/acetonitrile (58:42; pH, 5 ± 0.1) was eluted at a flow rate of 1.9 mL/min, and effluent was monitored at 227 nm using a UV detector. Quantitation was achieved by measurement of the peak area ratios of the drug to the internal standard. The pharmacokinetic parameters including the area under the plasma concentration–time curve

from zero to infinity ($AUC_{0-\infty}$), the apparent volume of distribution (V_d), systemic plasma clearance (CL), distribution half-life ($t_{1/2\alpha}$), elimination half-life ($t_{1/2\beta}$), and mean residence time (MRT) were calculated for each formulation by standard methods. WinNonlin software version 4.1 (Pharsight Corporation, California, USA) was used to analyze the pharmacokinetics parameters.

Statistical analysis

Data were expressed as means of three separate experiments and were compared by independent sample t-test for two groups, and one-way ANOVA followed by *post-hoc* for multiple groups. A *P*-value < 0.05 was considered statistically significant in all cases.

Results and discussion

Synthesis of RA-PF127 derivative

The synthesis of RA-PF127 derivative was carried out as shown in Fig.1 and identified by ^{1}H-NMR and FTIR analysis. ^{1}H-NMR spectrum of PF127 (Fig. 2A) revealed a signal around 1 ppm which was assigned to methyl groups of isopropyl repeating unit ($CH_2CHC\underline{H_3}O$) of PF127.The hydrogens of methylene groups of PF127 were observed around 3-4 ppm. As shown in Fig. 2B , peaks around 6-7 ppm attributed to the ethylene protons of the long alkene chain of RA, were observed in the spectrum of RA-PF127 (Fig. 2C), while no such peaks existed at the same chemical shift in the spectrum of PF127. The hydrogens of RA which are next to the acidic groups were shifted from 5.76 ppm in RA spectrum to 5.87 ppm in spectrum of RA-PF127 as the result of ester bond formation. Furthermore, the disappearance of the acidic proton of RA at 12 ppm denoted the lack of any unreacted RA in the final product. The coupling reaction between PF127 and RA was further confirmed by FTIR analysis. The FTIR spectra of PF127, RA, their physical mixture and the final product are shown in Fig 3. In the spectrum of PF127 (Fig. 3A), absorption bands at 1110 and 3468 cm^{-1} were assigned to C-O and O-H stretching vibration of PF127, respectively. The band around 2887-3000 cm^{-1} pertained to C-H aliphatic stretching vibration. In the spectrum of RA (Fig. 3B) the signal related to the stretching vibration of carbonyl group observed at 1684 cm^{-1}. This signal is shifted to 1693 cm^{-1} in the spectrum of RA-PF127 (Fig. 3D), which is due to C=O stretching vibration of newly formed ester group. Furthermore, the bands around 1566-1600 cm^{-1} representing C=C stretching vibration of RA and the band at 2887 cm^{-1} related to aliphatic chain of PF127, were observed in the spectrum of RA-PF127. All these results certified the successful synthesis of RA-PF127.

The degree of RA grafting to PF127 was determined by the peak areas of the methyl protons of isopropyl repeating unit of PF127 (chemical shift 1 ppm) and hydrogen of RA next to the carbonyl moiety

(chemical shift 5.87 ppm). The mole ratio of RA to PF127 in this experiment was calculated 3.14 from below equation:

$$DS = \frac{ntegral\ of\ signal\ at\ 5.87\ ppm\ \times 195}{Integral\ of\ signal\ at\ 1.00\ ppm}$$

Characteristics of mixed micelles

Fig. 4 shows the changes of fluorescence intensity ratios (I_1/I_3) against the logarithm of RA-PF127/TPGS in different weight ratios. The CMC of different formulations in deionized water are also listed in Table 1. The CMC values varied from 0.017 to 0.124 mg/mL and the data revealed that incorporation of TPGS increased the CMC of the micelles. Despite the unique advantages of TPGS such as anticancer activity and inhibition of p-gp, it has a high CMC value (0.12 mg/mL), which decreases the stability of micelles in physiological environment. Thus, till now, TPGS has been usually used together with other lipids or synthetic copolymers to form more stable micelles and the presence of TPGS in the micelles has greatly improved the drug encapsulation efficiency and stability of the micelles [31, 32] . In the current study we synthesized a new derivative of PF127 through the reaction with RA with much lower CMC value (0.017 mg/mL) compared to TPGS alone. The CMC values for RA-PF127/TPGS (7:3) and RA-PF127/TPGS (5:5) were found to be 0.042 and 0.034 mg/mL, respectively, which are much lower than those of low molecular weight surfactants in water (10^{-6}–10^{-4}M). This very small CMC values represent more resistance to the effects of dilution following injection to the blood circulation and therefore greater stability. Based on our results, the conjugation of RA to the PF127 and incorporation into the micellar structure increased the stability of the formulations. Furthermore, RA could synergistically enhance the therapeutic effect of PTX. Table 1 also listed the average sizes and zeta potentials of the lyophilized mixed micelles. The micellar sizes were significantly increased from 109.9 ± 8.2 nm for PF127-RA/TPGS (0:10) to 193.6 ± 19.8 nm for PF127-RA/TPGS (10:0) micelles which might result from the long hydrophobic chain of PF127. In a similar study, mixed micelles of PF105 and TPGS were prepared for delivery of camptothecin [31] . The average hydrodynamic diameters reported were 100 nm and were not significantly changed when different amounts of PF105 was incorporated in the micelles [31]. In the current study, the zeta potentials of the micelles varied from -10.4 to -13.9 mV and did not show any significant differences between the studied formulations. TEM images of PF127/TPGS (7:3) micelles (Fig. 5) revealed nanoparticles with spherical shape and approximately 130 nm sizes, which was similar to the results obtained by photon correlation spectroscopy.

Preparation and characterization of PTX-loaded micelles

As listed in Table 1, the size of PTX-loaded micelles was larger than those of the blank micelles which may be due to the drug loaded in the micellar core. The zeta potentials were reduced after the drug was loaded which could be attributed to the change of size and surface charge density of the micelles. The EEs of PTX in formulations were in the range of 10.1 %– 78.7 % which was the highest for RA-PF127/TPGS (5:5). Drug loading capacity of polymeric micelles mainly depends on hydrophobic interaction, miscibility of the drugs in the inner core of the micelles, and hydrophilic–lipophilic balance (HLB) of the copolymers [21] .The EEs of the drug in mixed micelles prepared from RA-PF127/TPGS (5:5) were 78.7 ± 1.66 % (w/w) compared to those of RA-PF127 micelles which were found to be 53.4 ± 9.3 % (w/w). This significant increase in drug loading capacity could be explained by high solubility of PTX in α-TS and strong hydrophobic interaction between the drug and bulk lipophilic portion of TPGS.

In vitro PTX release from RA-PF127/TPGS micelles

In vitro PTX release profiles from different formulations are shown in Fig. 6. From all the formulations, approximately 10–20 % of PTX was released within 8 h at 37 °C; afterwards, the release rate slowed down and were almost completed after 72 h for RA- PF127/TPGS (10:0) and RA- P127/TPGS (3:7). RA-PF127/TPGS (3:7) showed highest DE_{48h}% value of 48.69 ± 0.52% followed by RA-P127/TPGS (10:0) (45.74 ± 1.96 %) and RA-PF127/TPGS (7:3) (30.36 ± 1.04 %). The PTX release rates from RA-P127/TPGS (5:5) were significantly slower than other formulations with DE_{48}% of 28.36 ± 1.04 %. The enhanced sustained drug release behaviors observed by increasing the amount of TPGS could be explained by the strong hydrophobic interactions between PTX and the bulk lipophilic portion of TPGS molecules. However, 3: 7 micellar combinations resulted in very loose micelles (CMC value: 0.098) where easily dissociated in aqueous media and the release rate was significantly increased. In the majority of earlier published reports [33-35] , the release rate of PTX from polymeric micelles, especially in initial stages, was much faster than that of our developed micelles. In other similar studies, incorporation of TPGS to the micelles core significantly enhanced the loading of lipophilic drugs and reduced the drug release rates [24, 31] . In our previous work, we developed an amphiphilic derivative of chitosan for co-delivery of PTX and α-TS [21]. Similarly, incorporation of α-TS into the micelles enhanced hydrophobic interaction between PTX and the of micelles core to form a tightly packed hydrophobic core and sustained the drug release rate from the micelles.

Stability studies

The lyophilized PTX-loaded RA-PF127/TPGS with weight ratios of 7:3 and 5:5 were used in the stability studies. The freeze-dried PTX-loaded micelles were easily dissolved in water after 3-month storage at 4

°C. As shown in Table 2, PTX content of the 7:3 micellar combination had no significant change, although a slight decrease from 66.1% to 61.3 % was observed.

The average diameter of RA-PF127/TPGS 7:3 micelle increased from 157.5 to 201.1 nm. A significant decrease in PTX content was observed in RA-PF127/TPGS 5:5 micelle after 3 months storage ($p < 0.05$) which might result from the aggregation of the micelles during storage.

In vitro cellular uptake of RA-PF127/TPGS (3:7) micelles

The cellular uptake of RA-PF127/TPGS (7:3) micelles was examined to evaluate the penetration of the micelles into the cells. As shown in Fig. 7, a negligible fluorescence inside MCF-7 cells was detected at 2 h after incubation of cells with FITC/RA-PF127/TPGS (7:3). After 4 h, the obvious fluorescence intensity was observed which was enhanced with increasing incubation time up to 8 h, indicating that the cellular uptake of the micelles is a time-dependent process. As a control, no fluorescence inside MCF-7 cells was observed after the cells were incubated with FITC solution for 8h.

In vitro cytotoxicity studies

Fig. 8 compares cytotoxic effects of free PTX in DMSO, Stragen®, and the drugs-loaded micelles against MCF-7 cells. Stragen® and free PTX at equivalent doses showed similar cytotoxicity up to 0.352 µM against MCF-7 cells. However, at concentrations 0.586 to 2.345 µM, Stragen® exhibited significantly greater toxicity than free PTX ($P < 0.05$) which might be due to the cytotoxicity of its vehicle, Cremophor® EL. PTX-loaded mixed micelles exhibited the highest cytotoxicity amongst studied groups. The increased cytotoxicity of PTX-loaded RA-PF127/TPGS micelles could be associated with unique apoptosis-inducing properties of α-TS unimers of TPGS. The significant greater toxicity ($P < 0.05$) of empty RA-PF127/TPGS micelles compared to RA-PF127 at concentrations higher than 0.117 µM, could more imply the cytotoxic effect of TPGS. . Recently, we developed a novel polymeric micelles for co-delivery of PTX and α-TS to the cancer cells [21]. The results of cell culture studies on human ovarian cancer cells, SKOV3, demonstrated the synergistic cytotoxic effect between PTX and α-TS. In addition, TPGS through the inhibition of drug efflux pumps or P-gps, could facilitate delivery of PTX to the site of action, which is located in the nucleus. The empty RA-PF127 did not show any measurable toxicity at low concentrations (≤ 0.352 µM), however, the viability of the cells were significantly decreased as the drug concentrations increased from 0.586 µM to 2.34 µM. Moreover, PTX-loaded RA-PF127 micelles demonstrated significant ($P < 0.05$) cytotoxic effect compared to the free drug in the tested concentration ranges of PTX. This increased cytotoxicity might be explained as the result of RA-mediated PTX sensitization by inhibiting mitosis and the proliferation of cancer cells.

Pharmacokinetic studies results

The mean plasma concentration time profiles of PTX in blood after i.v. administration of PTX-loaded RA-PF127/TPGS (7:3) and Stregan® are shown in Fig. 9. The related pharmacokinetic parameters are also listed in Table 3. The decline in plasma concentration following i.v. administration of Stregan® and the micellar formulation is described by a two-compartment open model. The plasma concentrations of PTX-loaded mixed micelle were significantly lower than Stragen® injection at all sampling times. A rapid decline in distribution phase was observed after dosing with two preparations. In contrast, the elimination half-life of PTX-loaded RA-PF127/TPGS (7:3) (3.973 ± 0.341 h) was significantly ($p < 0.05$) longer than that of Stragen® (3.102 ± 0.356 h). Moreover, the MRT and V_d of PTX-loaded RA-PF127/TPGS micelle were significantly greater than those of Stragen® injection. The CL_s of PTX-loaded micelle (900.1 ± 123.2 mL/h/kg) was 2-fold higher than that of Stragen®. On the other hand, the AUC of micellar formulation (7.769 ± 0.976 µg h/mL) was 2.03 times lower than Stregan®. The AUC of PTX mainly depends on the distribution phase rate constant (α) and elimination phase (β) in plasma. The PTX-loaded RA-PF127/TPGS micelle was easily distributed in various tissues resulting in the lower plasma PTX concentrations which contributed to the lower calculated AUC values compared to Stragen®. The significant higher V_d of PTX-loaded mixed micelle (5.08 ± 1.01 L/Kg) compared to Stragen® (1.94 ± 0.25 L/Kg) also supported the observed lower AUC. For the micellar formulations, the dissociation dynamics of micelles below CMC dominate the β value. The micelles with a lower CMC value and stronger hydrophobic interactions have more thermodynamic stability. As they are less susceptible to disintegrate during blood dilution upon administration they can slow down the decrease of the drug concentration in the elimination phase, as a consequence they exhibit smaller ß value compared with the free drug (Emami et al., 2015). As shown in Table.3, the β value of the micellar formulation was approximately 1.9-fold smaller than that of stragen®, indicating high thermodynamic stability of the micelles. Furthermore, PTX in the micelles releasing from tissue to blood during metabolism may decrease the β value. In earlier published reports [36-38], the plasma AUC of PTX-loaded micelles has been much smaller than that of the free drug. A significant decline in AUC value suggests that the inner core of micelles with such a weak hydrophobic interaction could not efficiently entrap the drug. Our data demonstrated that these novel mixed micelles were stable in blood and could be used for the potential delivery of PTX and RA toward cancer cells.

Conclusion

In this study, RA was conjugated to PF127 via esterification process to yield. Afterward, RA-PF127 was used to form mixed micelles with TPGS for delivery of PTX into the cancer cells. The incorporation of TPGS as a part of micelle formation produced smaller particles with significant higher stability during

storage. The RA and TPGS moieties significantly increased the cytotoxic effect of PTX due to the synergistic cytotoxic effects and inhibition of p-gps. As demonstrated by pharmacokinetic studies in rats, PTX-loaded RA-PF127/TPGS (7:3) micelles displayed prolonged residence time in blood circulation and could be used for the potential delivery of PTX and RA toward cancer tumors.

Legends

Fig.1. synthetic scheme of RA-PF127 derivative.

Fig. 2. ^{1}H-NMR spectra of (A) PF127 in mixture of DMSO-d_6 and D_2O, (B) RA in DMSO- d_6, and (C) RA-PF127 DMSO-d_6.

Fig 3. FTIR spectra of (A) PF127, (B) RA, (C) physical mixture of RA and PF127, (D) RA-PF127,

Fig. 4. Plots of I_1/I_3 against the logarithm of RA-PF127/TPGS concentrations.

Fig 5. Transmission electron microscope (TEM) image of RA-PF127/TPGS (7:3) micelles.

Fig 6. *In vitro* drug-release profiles from mixed micelles with different weight ratios of the structural composition. Data represent the mean ± standard deviation (n = 3).

Fig 7. Visible and fluorescence images after cell exposure to 20 µg/mL FITC/RA-PF127/TPGS (7:3) micelles

Fig 8. *In vitro* cytotoxicity of various PTX containing formulations and blank micelles against MCF-7 cell line after 48 h incubation. Data are plotted as the mean ± standard deviation (n=3).

Stragen® at concentrations 0.582-2.345 exhibited greater toxicity than free PTX ($P < 0.05$)

PTX-loaded mixed micelles showed higher cytotoxicity compared to Stragen®, the free drug, and PTX-loaded RA-PF127 in all of the concentration ranges of PTX ($P < 0.05$)

RA-PF127/TPGS exhibited greater toxicity than RA-PF127 in concentration higher than 0.117 µM ($P<0.05$)

Fig 9. Mean concentration–time profiles of PTX in rat plasma after i.v. administration of Stragen® and PTX-loaded RA-PF127/TPGS (7:3) micelles. Each point represents the mean ± standard deviation (n =3).

TABLES

Table 1. Characteristics of blank and drug-loaded RA-PF127/TPGS mixed micelles

Table 2. Particle size, zeta potential, and entrapment efficiency of the lyophilized drug-loaded micelles before and after 3 months storage at 4 ºC.

Table 3. Pharmacokinetic parameters of PTX in blood for Stragen® and PTX-loaded RA-PF127/TPGS (7:3) (n = 5).

References

[1] Sledge G.W, Neuberg D, Bernardo P, el al. Phase III trial of doxorubicin, paclitaxel, and the combination of doxorubicin and paclitaxel as front-line chemotherapy for metastatic breast cancer: an intergroup trial (E1193), Journal of Clinical Oncology 21(4) (2003) 588-592.
[2] S. Carrick, S. Parker, C.E. Thornton, D. Ghersi, J. Simes, N. Wilcken, Single agent versus combination chemotherapy for metastatic breast cancer, The Cochrane Library (2009).
[3] Y.-J. Bang, E. Van Cutsem, A. Feyereislova, H.C. Chung, L. Shen, A. Sawaki, F. Lordick, A. Ohtsu, Y. Omuro, T. Satoh, Trastuzumab in combination with chemotherapy versus chemotherapy alone for treatment of HER2-positive advanced gastric or gastro-oesophageal junction cancer (ToGA): a phase 3, open-label, randomised controlled trial, The Lancet 376(9742) (2010) 687-697.
[4] W.-Y. Zhu, C.S. Jones, A. Kiss, K. Matsukuma, S. Amin, L.M. De Luca, Retinoic acid inhibition of cell cycle progression in MCF-7 human breast cancer cells, Experimental cell research 234(2) (1997) 293-299.
[5] Siddikuzzaman, C. Guruvayoorappan, V. Berlin Grace, All trans retinoic acid and cancer, Immunopharmacology and immunotoxicology 33(2) (2011) 241-249.
[6] K. Sano, T. Takayama, K. Murakami, I. Saiki, M. Makuuchi, Overexpression of retinoic acid receptor α in hepatocellular carcinoma, Clinical cancer research 9(10) (2003) 3679-3683.
[7] F.R. Khuri, J.J. Lee, S.M. Lippman, E.S. Kim, J.S. Cooper, S.E. Benner, R. Winn, T.F. Pajak, B. Williams, G. Shenouda, Randomized phase III trial of low-dose isotretinoin for prevention of second primary tumors in stage I and II head and neck cancer patients, Journal of the National Cancer Institute 98(7) (2006) 441-450.
[8] C. CLERICI, D. CASTELLANI, G. RUSSO, S. FIORUCCI, G. SABATINO, V. GIULIANO, G. GENTILI, O. MORELLI, P. RAFFO, M. BALDONI, Treatment with all-trans retinoic acid plus tamoxifen and vitamin E in advanced hepatocellular carcinoma, Anticancer research 24(2C) (2004) 1255-1260.
[9] R. Wang, H. Xiao, H. Song, Y. Zhang, X. Hu, Z. Xie, Y. Huang, X. Jing, Y. Li, Co-delivery of all-trans-retinoic-acid and cisplatin (IV) prodrug based on polymer–drug conjugates for enhanced efficacy and safety, Journal of Materials Chemistry 22(48) (2012) 25453-25462.

[10] J. Yao, L. Zhang, J. Zhou, H. Liu, Q. Zhang, Efficient simultaneous tumor targeting delivery of all-trans retinoid acid and paclitaxel based on hyaluronic acid-based multifunctional nanocarrier, Molecular pharmaceutics 10(3) (2013) 1080-1091.
[11] R. Sun, Y. Liu, S.-Y. Li, S. Shen, X.-J. Du, C.-F. Xu, Z.-T. Cao, Y. Bao, Y.-H. Zhu, Y.-P. Li, Co-delivery of all-trans-retinoic acid and doxorubicin for cancer therapy with synergistic inhibition of cancer stem cells, Biomaterials 37 (2015) 405-414.
[12] B. Ozpolat, G. Lopez-Berestein, P. Adamson, C. Fu, A.H. Williams, Pharmacokinetics of intravenously administered liposomal all-trans-retinoic acid (ATRA) and orally administered ATRA in healthy volunteers, J Pharm Pharm Sci 6(2) (2003) 292-301.
[13] C. Cho, K. Cho, I. Park, S. Kim, T. Sasagawa, M. Uchiyama, T. Akaike, Receptor-mediated delivery of all trans-retinoic acid to hepatocyte using poly (L-lactic acid) nanoparticles coated with galactose-carrying polystyrene, Journal of controlled release 77(1) (2001) 7-15.
[14] S.-J. Lim, C.-K. Kim, Formulation parameters determining the physicochemical characteristics of solid lipid nanoparticles loaded with all-trans retinoic acid, International journal of pharmaceutics 243(1) (2002) 135-146.
[15] G.A. Castro, R.L. Oréfice, J.M. Vilela, M.S. Andrade, L.A. Ferreira, Development of a new solid lipid nanoparticle formulation containing retinoic acid for topical treatment of acne, Journal of microencapsulation 24(5) (2007) 395-407.
[16] M. Narvekar, H.Y. Xue, H.L. Wong, A novel hybrid delivery system: polymer-oil nanostructured carrier for controlled delivery of highly lipophilic drug all-trans-retinoic acid (ATRA), International journal of pharmaceutics 436(1) (2012) 721-731.
[17] L. Hou, J. Yao, J. Zhou, Q. Zhang, Pharmacokinetics of a paclitaxel-loaded low molecular weight heparin-all-trans-retinoid acid conjugate ternary nanoparticulate drug delivery system, Biomaterials 33(21) (2012) 5431-5440.
[18] J. Zhang, J. Han, X. Zhang, J. Jiang, M. Xu, D. Zhang, J. Han, Polymeric nanoparticles based on chitooligosaccharide as drug carriers for co-delivery of all-trans-retinoic acid and paclitaxel, Carbohydrate polymers 129 (2015) 25-34.
[19] A. Pitto-Barry, N.P. Barry, Pluronic® block-copolymers in medicine: from chemical and biological versatility to rationalisation and clinical advances, Polymer Chemistry 5(10) (2014) 3291-3297.
[20] Z. Zhang, S. Tan, S.-S. Feng, Vitamin E TPGS as a molecular biomaterial for drug delivery, Biomaterials 33(19) (2012) 4889-4906.
[21] J. Emami, M. Rezazadeh, M. Rostami, F. Hassanzadeh, H. Sadeghi, A. Mostafavi, M. Minaiyan, A. Lavasanifar, Co-delivery of paclitaxel and α-tocopherol succinate by novel chitosan-based polymeric micelles for improving micellar stability and efficacious combination therapy, Drug development and industrial pharmacy 41(7) (2015) 1137-1147.
[22] H. Zhu, H. Chen, X. Zeng, Z. Wang, X. Zhang, Y. Wu, Y. Gao, J. Zhang, K. Liu, R. Liu, Co-delivery of chemotherapeutic drugs with vitamin E TPGS by porous PLGA nanoparticles for enhanced chemotherapy against multi-drug resistance, Biomaterials 35(7) (2014) 2391-2400.
[23] P. Xu, Q. Yin, J. Shen, L. Chen, H. Yu, Z. Zhang, Y. Li, Synergistic inhibition of breast cancer metastasis by silibinin-loaded lipid nanoparticles containing TPGS, International journal of pharmaceutics 454(1) (2013) 21-30.
[24] K.K. Gill, A. Kaddoumi, S. Nazzal, Mixed micelles of PEG 2000-DSPE and vitamin-E TPGS for concurrent delivery of paclitaxel and parthenolide: Enhanced chemosenstization and antitumor efficacy against non-small cell lung cancer (NSCLC) cell lines, European journal of pharmaceutical sciences 46(1) (2012) 64-71.
[25] H.-J. Youk, E. Lee, M.-K. Choi, Y.-J. Lee, J.H. Chung, S.-H. Kim, C.-H. Lee, S.-J. Lim, Enhanced anticancer efficacy of α-tocopheryl succinate by conjugation with polyethylene glycol, Journal of controlled release 107(1) (2005) 43-52.
[26] Y. Mi, Y. Liu, S.-S. Feng, Formulation of docetaxel by folic acid-conjugated d-α-tocopheryl polyethylene glycol succinate 2000 (Vitamin E TPGS 2k) micelles for targeted and synergistic chemotherapy, Biomaterials 32(16) (2011) 4058-4066.

[27] J. Emami, M. Rezazadeh, F. Hasanzadeh, H. Sadeghi, A. Mostafavi, M. Minaiyan, M. Rostami, N. Davies, Development and in vitro/in vivo evaluation of a novel targeted polymeric micelle for delivery of paclitaxel, International journal of biological macromolecules 80 (2015) 29-40.
[28] J. Emami, M. Rezazadeh, H. Sadeghi, K. Khadivar, Development and optimization of transferrin-conjugated nanostructured lipid carriers for brain delivery of paclitaxel using Box–Behnken design, Pharmaceutical development and technology 22(3) (2017) 370-382.
[29] A. Mostafavi, J. Emami, J. Varshosaz, N.M. Davies, M. Rezazadeh, Development of a prolonged-release gastroretentive tablet formulation of ciprofloxacin hydrochloride: pharmacokinetic characterization in healthy human volunteers, International journal of pharmaceutics 409(1) (2011) 128-136.
[30] J. Emami, M. Rezazadeh, J. Varshosaz, Formulation of LDL targeted nanostructured lipid carriers loaded with paclitaxel: a detailed study of preparation, freeze drying condition, and in vitro cytotoxicity, Journal of Nanomaterials 2012 (2012) 3.
[31] Y. Gao, L.B. Li, G. Zhai, Preparation and characterization of Pluronic/TPGS mixed micelles for solubilization of camptothecin, Colloids and Surfaces B: Biointerfaces 64(2) (2008) 194-199.
[32] V. Saxena, M.D. Hussain, Polymeric mixed micelles for delivery of curcumin to multidrug resistant ovarian cancer, Journal of biomedical nanotechnology 9(7) (2013) 1146-1154.
[33] W.Y. Seow, J.M. Xue, Y.-Y. Yang, Targeted and intracellular delivery of paclitaxel using multi-functional polymeric micelles, Biomaterials 28(9) (2007) 1730-1740.
[34] W. Zhang, Y. Shi, Y. Chen, J. Ye, X. Sha, X. Fang, Multifunctional Pluronic P123/F127 mixed polymeric micelles loaded with paclitaxel for the treatment of multidrug resistant tumors, Biomaterials 32(11) (2011) 2894-2906.
[35] Y. Tao, J. Xu, M. Chen, H. Bai, X. Liu, Core cross-linked hyaluronan-styrylpyridinium micelles as a novel carrier for paclitaxel, Carbohydrate Polymers 88(1) (2012) 118-124.
[36] S.C. Kim, D.W. Kim, Y.H. Shim, J.S. Bang, H.S. Oh, S.W. Kim, M.H. Seo, In vivo evaluation of polymeric micellar paclitaxel formulation: toxicity and efficacy, Journal of Controlled Release 72(1) (2001) 191-202.
[37] J. Liu, H. Li, D. Chen, X. Jin, X. Zhao, C. Zhang, Q. Ping, In vivo evaluation of novel chitosan graft polymeric micelles for delivery of paclitaxel, Drug delivery 18(3) (2011) 181-189.
[38] C. Zhang, G. Qu, Y. Sun, X. Wu, Z. Yao, Q. Guo, Q. Ding, S. Yuan, Z. Shen, Q. Ping, Pharmacokinetics, biodistribution, efficacy and safety of N-octyl-O-sulfate chitosan micelles loaded with paclitaxel, Biomaterials 29(9) (2008) 1233-1241.

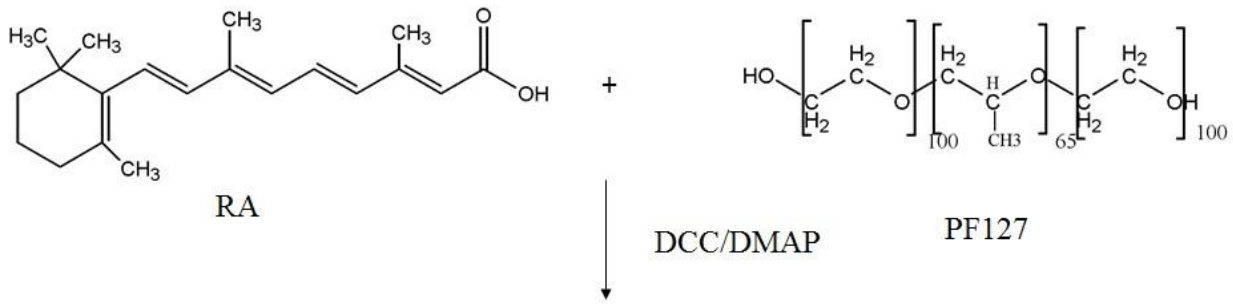

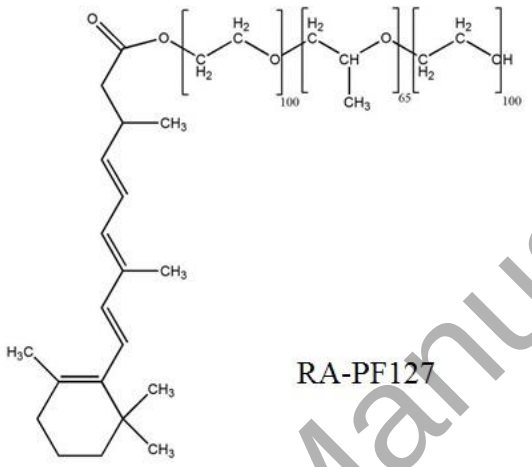

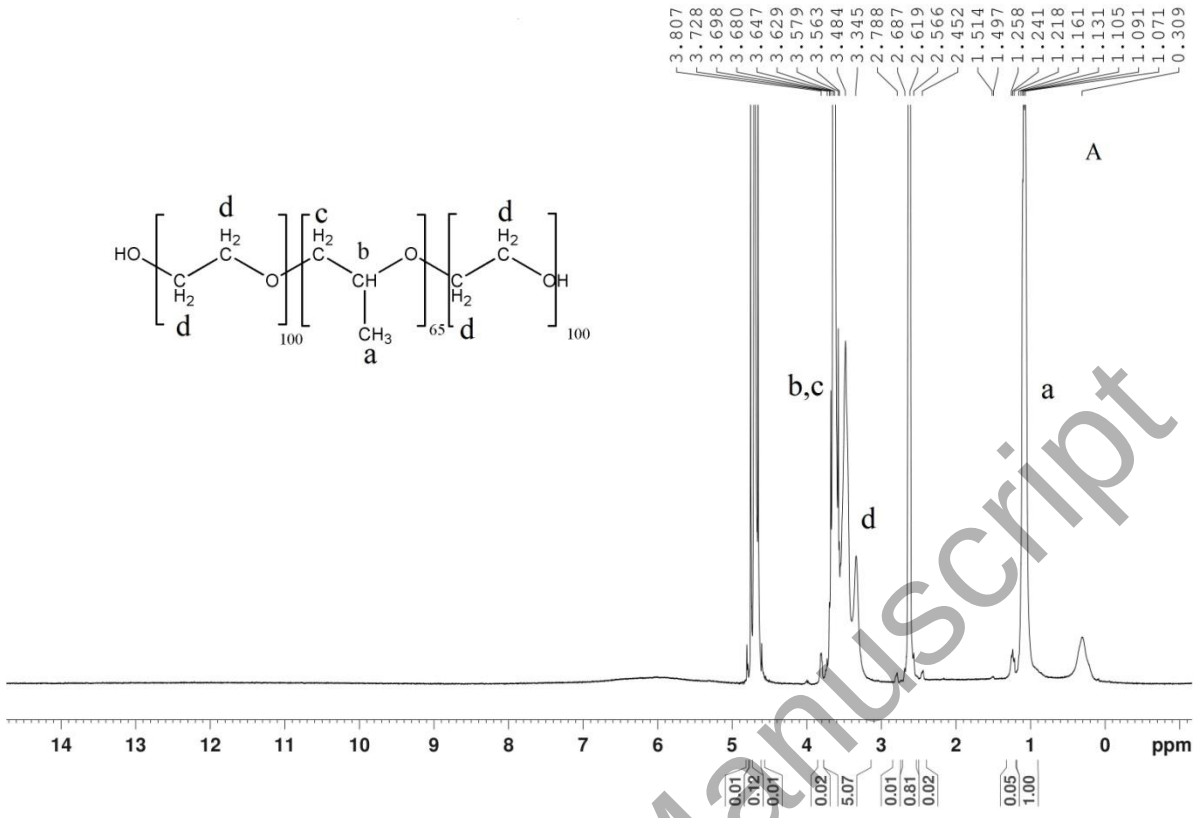

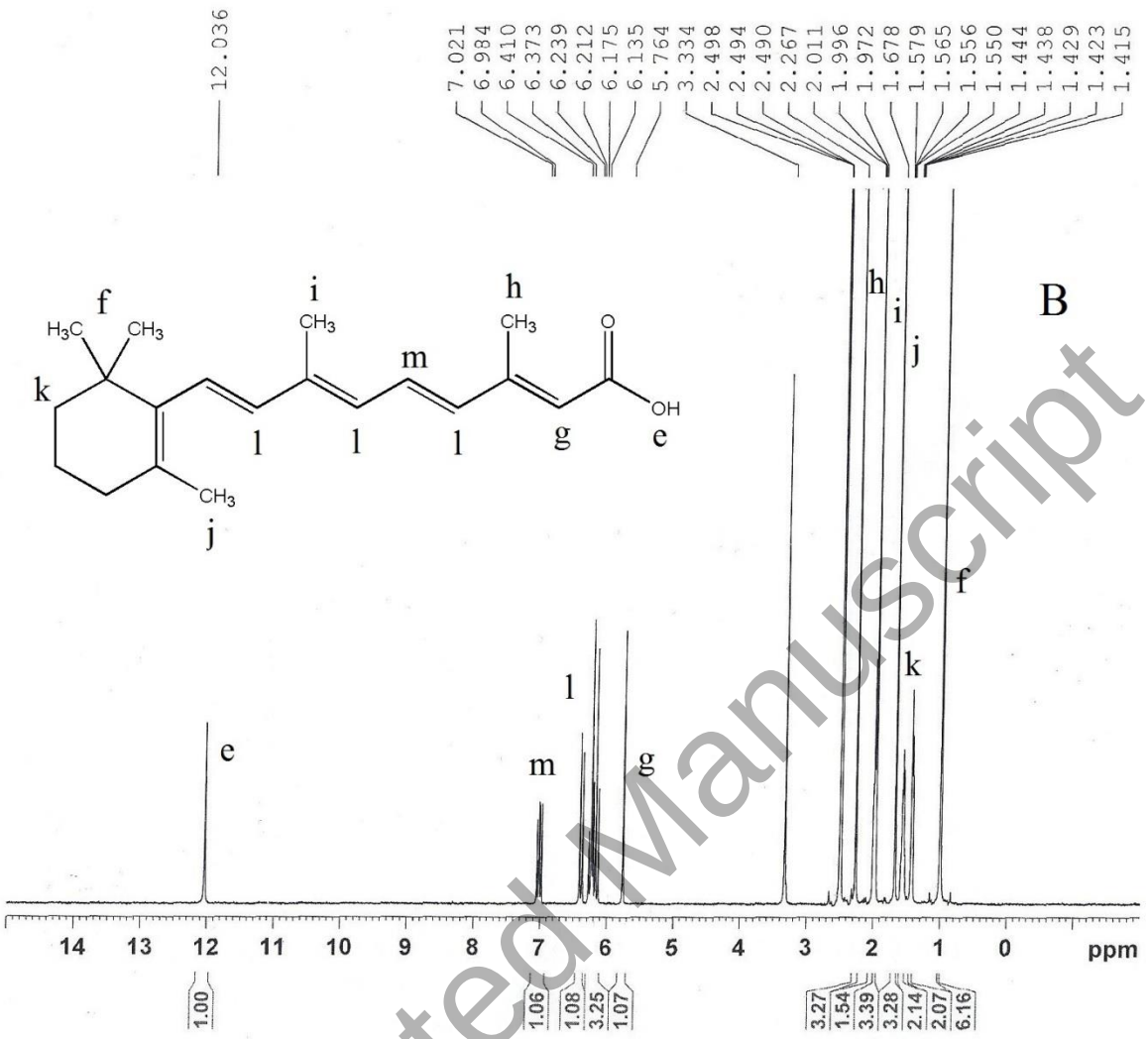

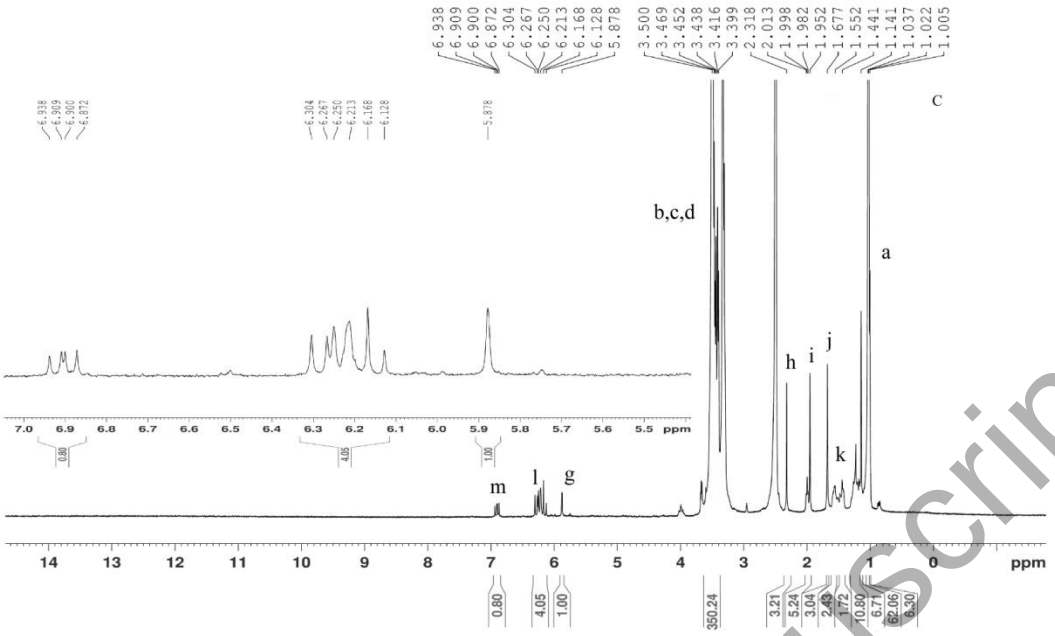

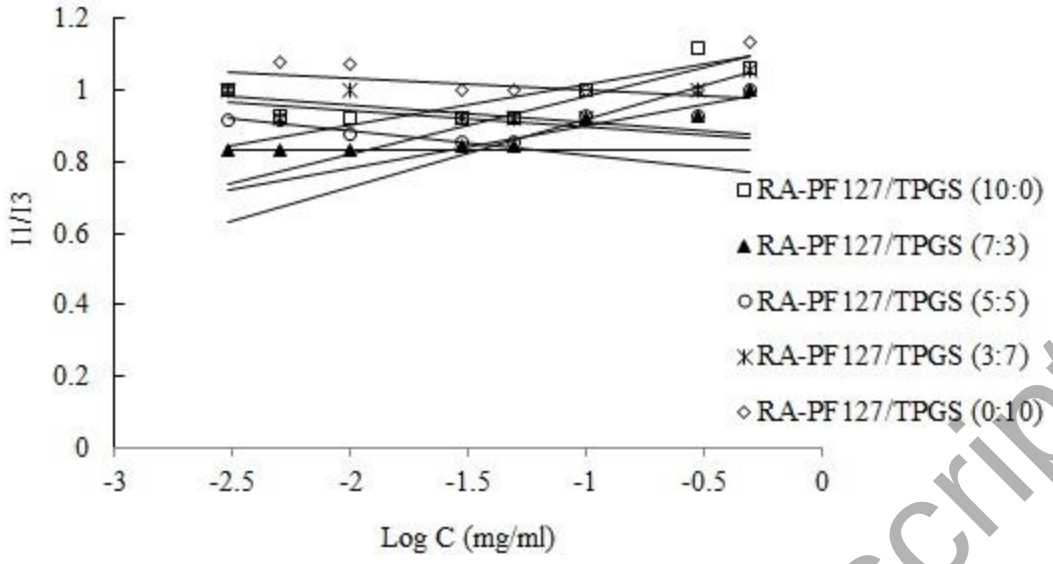

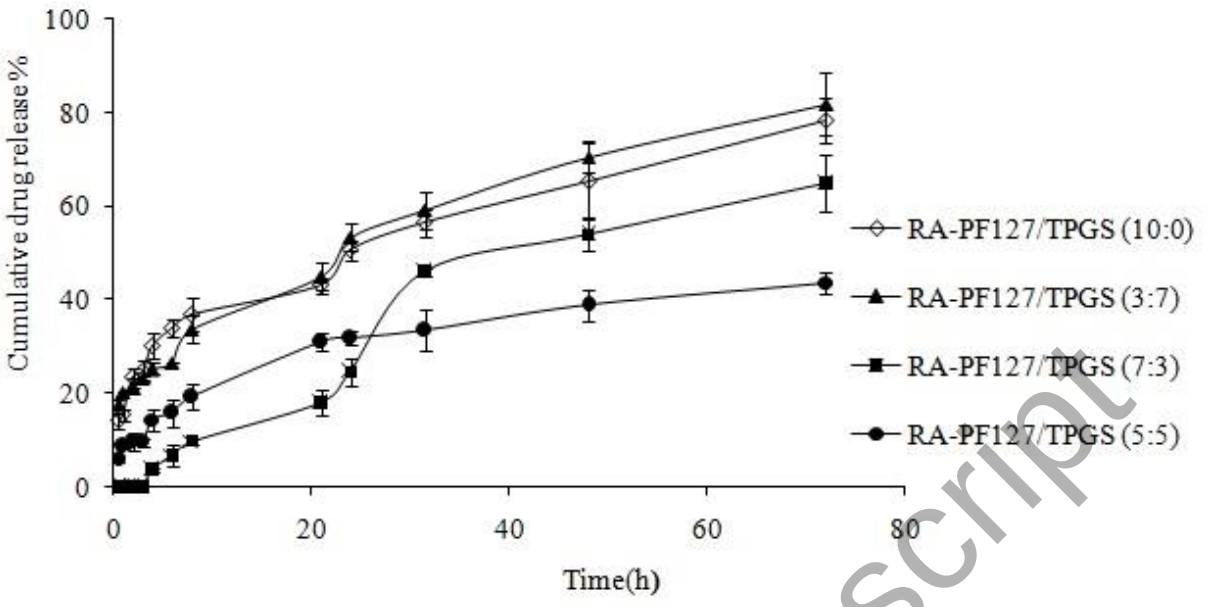

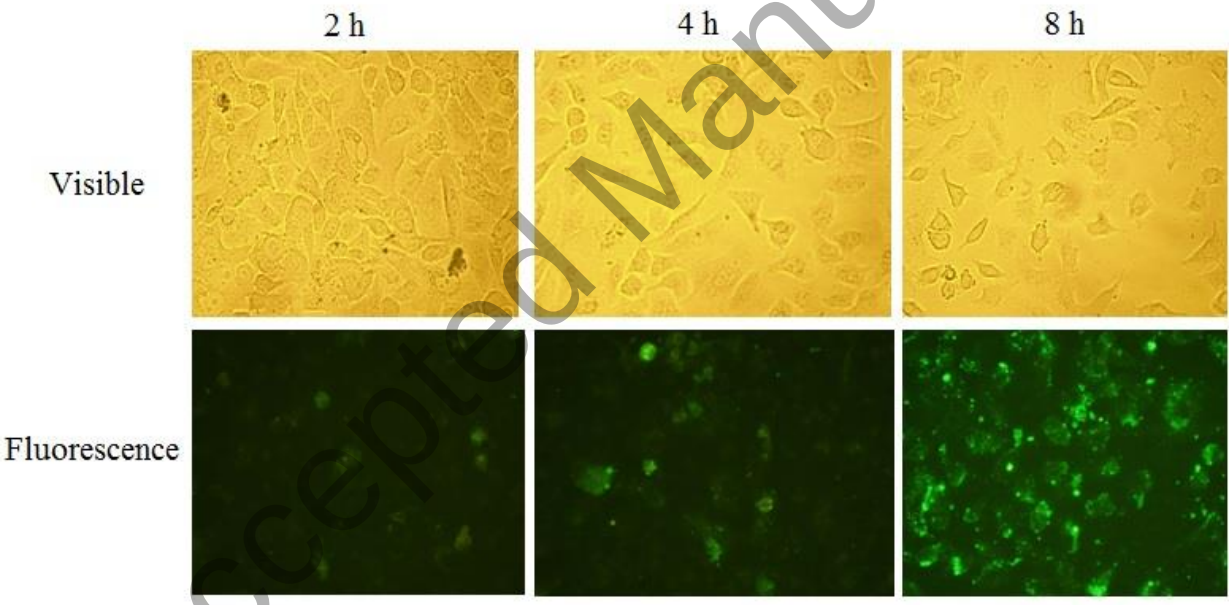

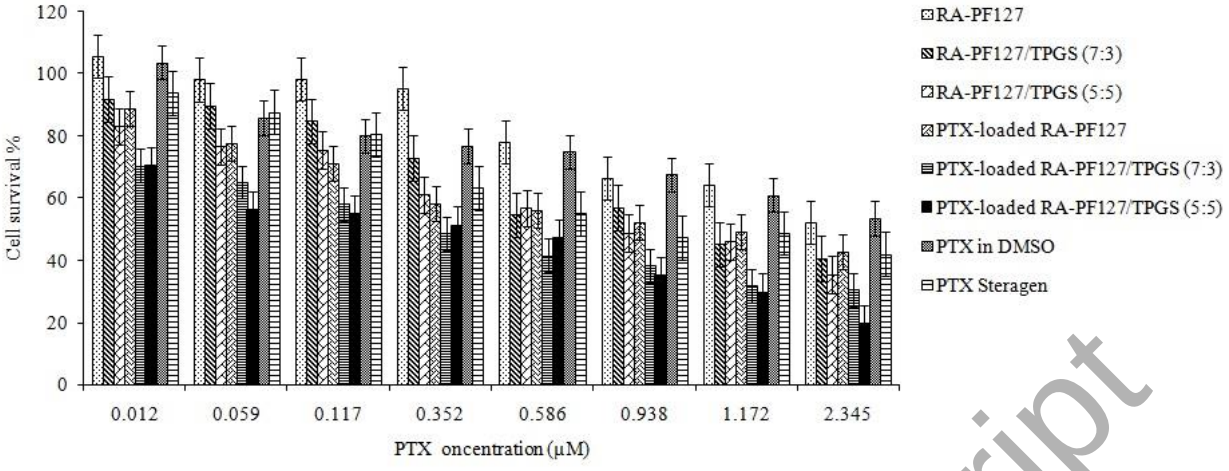

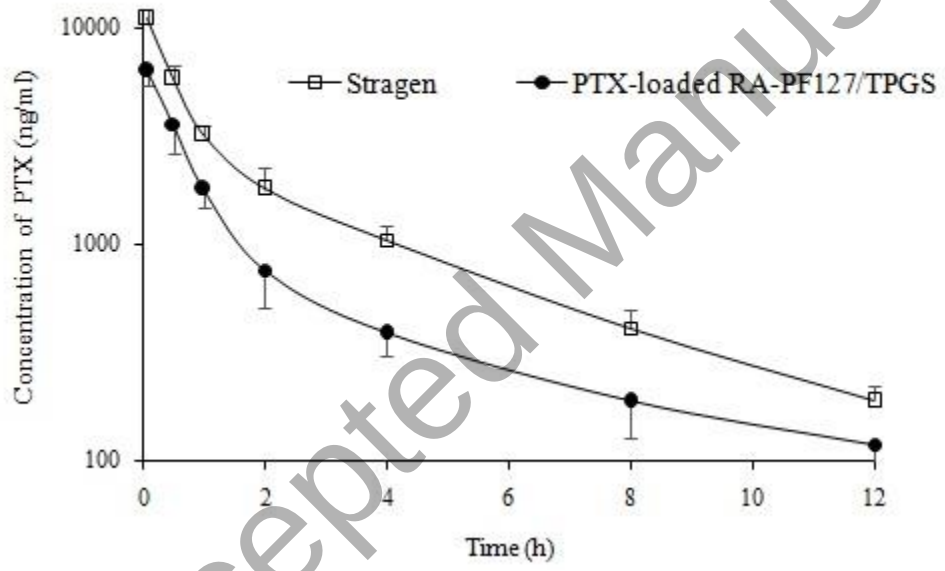

Table 1

formulations	CMC (mg/mL)	Micellar size (nm)	Zeta potential (mV)
PF127-RA/TPGS (10:0)	0.017	193.6 ± 19.8	-11.6 ± 1.4
PF127-RA /TPGS (7:3)	0.042	155.7 ± 16.3	-13.9 ± 3.7
PF127-RA /TPGS (5:5)	0.034	135.9 ± 9.1*	-10.8 ± 1.5
PF127-RA /TPGS (3:7)	0.098	144.0 ± 10.4*	-12.5 ± 3.1
PF127-RA /TPGS (0:10)	0.124	109.9 ± 8.2*	-10.4 ± 2.9
	EE % (DL %)	Micellar size (nm)	Zeta potential (mV)
PTX/ PF127-RA/TPGS(10:0)	53.4 ± 9.3 (11.7 ± 2.0)	223.5 ± 12.2	-7.3 ± 2.1
PTX/PF127RA/TPGS (7:3)	*61.3 ± 0.5 (13.5 ± 0.02)	157.5 ± 20.1	-9.6 ±1.1
PTX/PF127-RA/TPGS(5:5)	*78.7 ±1.66 (17.3 ± 0.3)	144.5 ± 14.7	-9.2 ± 2.6
PTX/PF127/TPGS (3:7)	51.0 ± 3.9 (11.2 ± 0.9)	172.1 ± 11.1	-8.2 ± 0.7
PTX/PF127/TPGS (0:10)	*10.1 ± 1.1 (2.2 ± 0.2)	102.6 ±11.61	-5.3 ± 0.5

EE: entrapment efficiency
DL: drug loading
*P value ≤ 0.05 compared to PF127-RA/TPGS (10:0)

Table 2

Formulation (storage time)	Particle size	Zeta potential	EE of PTX (%w/w)
PTX-loaded RA-PF127/TPGS 7:3 micelle (0 day)	157.5 ± 20.1*	-9.6 ± 1.1	61.3 ± 0.5
PTX-loaded RA-PF127/TPGS 7:3 micelle (3 months)	201.1 ± 25.7	-6.6 ± 0.4	66.1 ± 9.1
PTX-loaded RA-PF127/TPGS 5:5 micelle (0 day)	144.5 ± 14.7	-9.2 ± 2.6	78.7 ± 1.6*
PTX-loaded RA-PF127/TPGS 5:5 micelle (3 months)	175.5 ± 17.4	-6.7 ± 0.7	51.5 ± 0.5

* P<0.05
EE: Entrapment Efficiency

Table 3.

Parameters	Stragen®	PTX-loaded RA-PF127/TPGS (7:3)
α (1/h)	2.151± 0.332	2.565± 0.693
ß (1/h)	0.223± 0.041	0.177± 0.025*
V_d(L/kg)	1.946± 0.251	5.080± 1.013*
$T_{1/2\alpha}$ (h)	0.312± 0.061	0.278± 0.032
$T_{1/2ß}$(h)	3.102± 0.356	3.973 ±0.341*
Cl (ml/h/kg)	446.6± 72.45	900.1± 123.2*
AUC $_{(0-\infty)}$(µg h/ml)	15.78± 2.152	7.769± 0.978*
MRT $_{(0-\infty)}$ (h)	3.205± 0.293	3.933 ± 0.205*

Data represent mean value ± SD n=3
*P< 0.05 compared with Stragen®
α: Rate constant of distribution phase
ß: Rate constant of elimination phase
V_d:Apparent volume of distribution
$T_{1/2\alpha}$: Apparent plasma half-life of distribution phase
$T_{1/2ß}$: Apparent plasma half-life of elimination phase
CL: total body clearance
AUC $_{(0-\infty)}$: the area under the plasma concentration-time curve from time 0 to time infinity
MRT $_{(0-\infty)}$: mean residence time from time 0 to time infinity,